



Sodium channel $\beta 1$ subunit mutations associated with Brugada syndrome and cardiac conduction disease in humans

Hiroshi Watanabe,^{1,2} Tamara T. Koopmann,³ Solena Le Scouarnec,^{4,5,6} Tao Yang,¹ Christiana R. Ingram,¹ Jean-Jacques Schott,^{4,5,6,7} Sophie Demolombe,^{4,5,6} Vincent Probst,^{4,5,6,7} Frédéric Anselme,⁸ Denis Escande,^{4,5,6,7} Ans C.P. Wiesfeld,⁹ Arne Pfeufer,^{10,11} Stefan Kääh,¹² H.-Erich Wichmann,^{11,12} Can Hasdemir,¹³ Yoshifusa Aizawa,² Arthur A.M. Wilde,³ Dan M. Roden,¹ and Connie R. Bezzina³

¹Department of Medicine and Pharmacology, Vanderbilt University School of Medicine, Nashville, Tennessee, USA. ²Division of Cardiology, Niigata University Graduate School of Medical and Dental Sciences, Niigata, Japan. ³Heart Failure Research Center, Department of Experimental Cardiology, Academic Medical Center, University of Amsterdam, Amsterdam, The Netherlands. ⁴INSERM, UMR915, l'institut du thorax, Nantes, France. ⁵Université de Nantes, Nantes, France. ⁶CNRS ERL3147, Nantes, France. ⁷CHU Nantes, l'institut du thorax, Service de Cardiologie, Nantes, France. ⁸CHU Rouen, Département de Cardiologie, Rouen, France. ⁹Department of Cardiology, Thoraxcenter, University Medical Center Groningen, Groningen, The Netherlands. ¹⁰Institut für Humangenetik, Technical University of Munich, Munich, Germany. ¹¹Helmholtz Zentrum Munich, German Research Center for Environmental Health, Neuherberg, Germany. ¹²Department of Medicine I, Ludwig-Maximilians-University Munich, Klinikum Großhadern, Munich, Germany. ¹³Department of Cardiology, Ege University School of Medicine, Izmir, Turkey.

Brugada syndrome is a genetic disease associated with sudden cardiac death that is characterized by ventricular fibrillation and right precordial ST segment elevation on ECG. Loss-of-function mutations in *SCN5A*, which encodes the predominant cardiac sodium channel α subunit $\text{Na}_v1.5$, can cause Brugada syndrome and cardiac conduction disease. However, *SCN5A* mutations are not detected in the majority of patients with these syndromes, suggesting that other genes can cause or modify presentation of these disorders. Here, we investigated *SCN1B*, which encodes the function-modifying sodium channel $\beta 1$ subunit, in 282 probands with Brugada syndrome and in 44 patients with conduction disease, none of whom had *SCN5A* mutations. We identified 3 mutations segregating with arrhythmia in 3 kindreds. Two of these mutations were located in a newly described alternately processed transcript, $\beta 1B$. Both the canonical and alternately processed transcripts were expressed in the human heart and were expressed to a greater degree in Purkinje fibers than in heart muscle, consistent with the clinical presentation of conduction disease. Sodium current was lower when $\text{Na}_v1.5$ was coexpressed with mutant $\beta 1$ or $\beta 1B$ subunits than when it was coexpressed with WT subunits. These findings implicate *SCN1B* as a disease gene for human arrhythmia susceptibility.

Introduction

Voltage-gated sodium channels are critical for the generation and propagation of the cardiac action potential, and mutations in *SCN5A*, the gene encoding the major pore-forming sodium channel α subunit in the heart ($\text{Na}_v1.5$), cause multiple cardiac arrhythmia syndromes (1–4). Mutations producing enhanced inward current during the course of the action potential plateau, often as a consequence of destabilized fast inactivation of the channel, cause long QT syndrome type 3 (LQT3; OMIM 603830) (1). On the other hand, a reduction in sodium current leads to cardiac conduction disease, which may be progressive (OMIM 113900) (2, 3), and Brugada syndrome (OMIM 601144), characterized by ST segment elevation in the right precordial leads (V1 to V3) of the 12-lead ECG and episodes of ventricular fibrillation (4). Multiple mechanisms have been described that reduce sodium current in these syndromes, including altered gating of the channel or reduced cell-surface expression (5). In addition, mutations in *SCN5A* may manifest with an overlap of these different phenotypes (6–10). However, mutations in *SCN5A* are found in fewer than 30% of patients with Brugada syndrome, indicating involvement of other genes (11). A mutation in the glycerol-3-phosphate dehydrogenase 1-like gene (*GPD1L*) has recently been

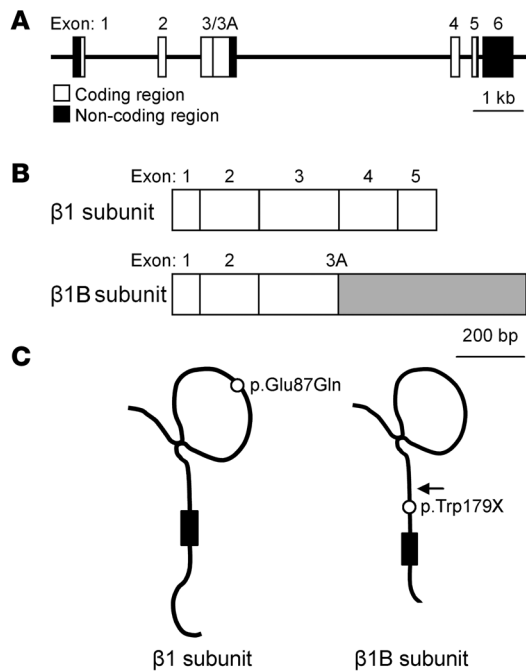
reported in a large kindred with Brugada syndrome (12); however, *GPD1L* mutations are rare in Brugada syndrome (13). Antzelevitch et al. have recently reported mutations in the gene encoding the L-type calcium channel (*CACNA1C*) or its $\beta 2b$ subunit (*CACNB2b*) in Brugada syndrome patients with unusually short QT intervals (14), but the frequency of these defects as a cause for more-typical Brugada syndrome is unknown. *SCN5A* mutations are also not identified in the majority of patients with cardiac conduction disease (15).

Sodium channels are multisubunit protein complexes composed not only of pore-forming α subunits but also of multiple other protein partners including auxiliary function-modifying β subunits (16, 17). In humans, 4 sodium channel β subunits ($\beta 1$ to $\beta 4$, encoded by *SCN1B* to *SCN4B*) have been identified, and they share a common predicted protein topology: a large extracellular N-terminal domain (including an immunoglobulin-like domain), a single transmembrane segment, and an intracellular C-terminal domain (16). Functions attributed to β subunits include an increase in sodium channel expression at the cell surface, modulation of channel gating and voltage dependence, and a role in cell adhesion and recruitment of cytosolic proteins such as ankyrin-G (16).

The $\beta 1$ transcript arises from splicing of exons 1–5 of the *SCN1B* gene (Figure 1, A and B). More recently, a second transcript has been described, arising from splicing of exons 1–3 with retention of a segment of intron 3 (termed exon 3A), leading to an alternate 3' sequence

Conflict of interest: The authors have declared that no conflict of interest exists.

Citation for this article: *J. Clin. Invest.* 118:2260–2268 (2008). doi:10.1172/JCI33891.

**Figure 1**

Structure of $\beta 1$ and $\beta 1B$ subunits. (A) Genomic structure of *SCN1B*. (B) Extension of exon 3 (c.208–458) into intron 3 creates a novel 3' end of the transcript (exon 3A, c.208–978) and generates an alternate transcript encoding $\beta 1B$. The gray region indicates the unique sequence of exon 3A. (C) Predicted topology of $\beta 1$ and $\beta 1B$. The $\beta 1B$ protein has unique juxtamembrane, transmembrane, and intracellular domains. The arrow indicates the initial amino acid of the $\beta 1B$ -specific segment. Circles indicate the locations of the mutations.

(Figure 1, A and B) (18, 19). This latter transcript encodes the $\beta 1B$ subunit, which, in spite of the different 3' sequence, has a predicted protein topology similar to that of $\beta 1$ (Figure 1C) (19). The $\beta 1B$ subunit has been shown to increase a neuronal sodium current ($Na_v1.2$) (19), but its effects on $Na_v1.5$ current have not yet been investigated, although $\beta 1$ and $\beta 1B$ are both expressed in heart (19, 20).

Since loss-of-function $Na_v1.5$ mutations cause conduction disease and Brugada syndrome, one could envision that mutations in sodium channel β subunits could also underlie these disorders by decreasing sodium current. Therefore, we tested the hypothesis that mutations in *SCN1B* coding sequences, for either $\beta 1$ or $\beta 1B$, underlie cases of conduction disease and Brugada syndrome. We identified 3 mutations segregating with arrhythmia in 3 kindreds, and 2 of the mutations were located in the newly described $\beta 1B$ transcript. Both $\beta 1$ and $\beta 1B$ transcripts were expressed in the human heart and were abundant in Purkinje fibers that play a critical role in electric pulse conduction in heart. Electrophysiologic study of heterologously expressed sodium channels revealed loss of sodium current with mutant subunits.

Results

Mutation analysis and clinical data. We screened 282 probands with Brugada syndrome and 44 with conduction disease for mutations in exons 1–5 of *SCN1B* encoding the $\beta 1$ subunit and in exon 3A retained in the $\beta 1B$ transcript (Figure 1, A and B). *SCN5A* coding region mutations had been previously excluded in all 326 subjects. Three variants were identified in probands and family members (Figure 2A). These variants were absent in 1,404 population controls (see Methods).

A missense mutation, c.259G→C (Figure 2B) in exon 3, resulting in p.Glu87Gln within the extracellular immunoglobulin loop of the protein (Figure 1C) was identified in a Turkish kindred affected by conduction disease (family 1; Figure 2A). Alignment of the $\beta 1$ subunit amino acid sequence from multiple species demonstrated that Glu87 is highly conserved, supporting the importance of glutamate at this position (Figure 2C). The proband was a

50-year-old white Turkish female (II-1) who presented with palpitations and dizziness. Physical examination and echocardiography were normal, and her ECG showed complete left bundle branch block. A clinical electrophysiological study revealed a prolonged His-ventricle interval of 80 ms and inducible atrioventricular nodal reentrant tachycardia; complete atrioventricular block occurred following atrial programmed stimulation and during induced tachycardia. A dual-chamber pacemaker was implanted with resolution of symptoms. The same mutation was found in her brother (II-3), who had bifascicular block (right bundle branch block and left anterior hemiblock), and her mother (I-2), who had a normal ECG. There was no family history of syncope, sudden cardiac death, or epilepsy.

A nonsense mutation, c.536G→A in exon 3A (Figure 1B and Figure 2D), was identified in a French kindred affected with Brugada syndrome and conduction disease (family 2; Figure 2A). This mutation results in p.Trp179X and is predicted to generate a prematurely truncated protein lacking the membrane-spanning segment and intracellular portion of the protein (Figure 1C). The proband was a 53-year-old white male (II-4) who presented with chest pain. Physical examination, echocardiography, and coronary angiography were normal. His ECG showed ST segment elevation typical of Brugada syndrome and conduction abnormalities (prolonged PR interval of 220 ms and left anterior hemiblock; Figure 2E) (21). Ventricular fibrillation was induced by programmed electrical stimulation in basal state (in the absence of drugs). The same mutation was detected in his brother (II-1), nephew (III-1), and sister (II-2). The brother had no palpitations or history of syncope. His baseline ECG showed left anterior hemiblock and minor ST segment elevation suggestive of Brugada syndrome at baseline (type II saddleback abnormality; ref. 21); with flecainide challenge, the ST segment elevation was further exaggerated but did not meet criteria for a diagnostic (type I) pattern. The nephew had right bundle branch block and type II Brugada syndrome ECG after flecainide challenge, and the sister had a normal ECG and a negative flecainide test. There was no family history of tachyarrhythmias, syncope, sudden cardiac death, or epilepsy.

A different nonsense mutation, c.537G→A in exon 3A (Figure 2D), resulting in p.Trp179X, affecting the same codon as in family 2, was identified in a Dutch kindred (family 3; Figure 2A). The proband was a 17-year-old white female (II-1). Physical examination and echocardiography were normal, and a flecainide test for Brugada syndrome was negative. Her ECG showed right bundle branch block and prolonged PR interval of 196 ms (normal upper limit in teenagers, 180 ms) (22). The same mutation was found in her father (I-1), with normal ECG and negative flecainide test. The family history was negative for syncope, sudden cardiac death, or epilepsy.

$\beta 1$ and $\beta 1B$ transcript expression. To confirm and extend previous reports that $\beta 1B$ is expressed in brain, heart, skeletal muscle, and other organs (19), we used quantitative real-time PCR in nondiseased

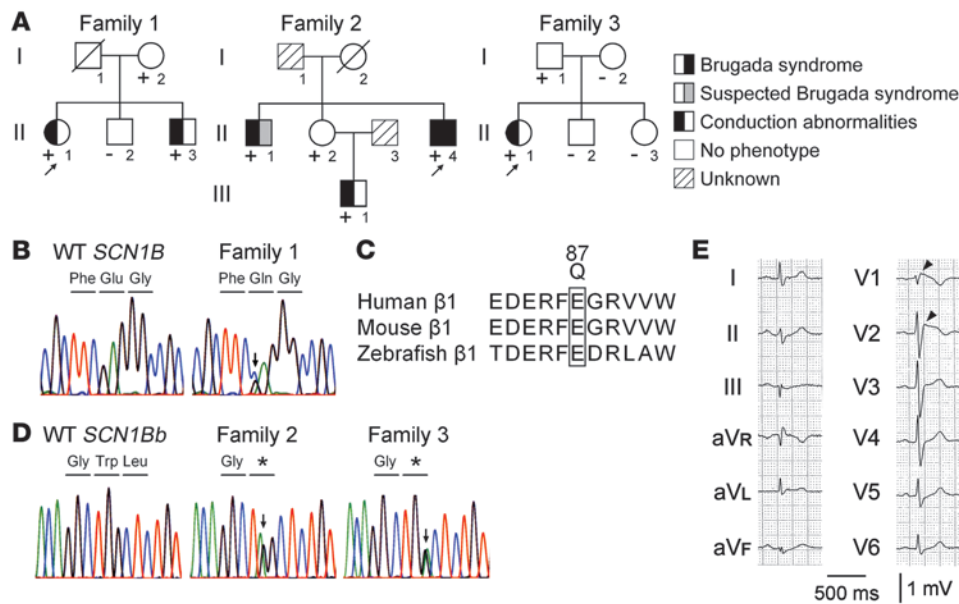


Figure 2
SCN1B mutations found in patients with Brugada syndrome and conduction disease. (A) Pedigrees and phenotypes of the families affected by Brugada syndrome and/or conduction disease. Individuals carrying the mutation are indicated (+). Individuals who tested negative for the mutation are indicated (-). Individuals I-1 from family 1; and I-1, I-2, and II-3 from family 2 did not undergo genetic testing. Arrows indicate probands. (B) The c.259G→C mutation in *SCN1B* resulting in p.Glu87Gln found in family 1. (C) Alignment of β1 across species showing the high conservation of Glu87. (D) The c.536G→A (middle) and c.537G→A (right) mutations in exon 3A of β1B, both resulting in p.Trp179X found in families 2 and 3, respectively. (E) Twelve-lead ECG from the proband of family 2 (II-4). The arrowheads indicate ST-segment elevation typical of Brugada syndrome.

human heart. Both β1 and β1B transcripts were detected in right and left ventricles and in Purkinje fibers (Figure 3). The β1 transcript level was higher in Purkinje fibers (which make up the conduction system in the ventricle) than left- (2.4-fold; $P < 0.05$) and right-ventricular (1.6-fold; $P = \text{NS}$) free walls. β1B transcript levels showed an even greater difference: Purkinje fibers versus left- (4.8-fold; $P < 0.001$) and right-ventricular (3.7-fold; $P < 0.001$) free walls. Levels of both transcripts were also slightly (but not statistically significantly) higher in right- versus left-ventricular free wall (1.5-fold and 1.3-fold for β1 and β1B transcripts, respectively).

Cellular electrophysiology. The effects of mutant and WT β1 and β1B variants on $\text{Na}_v1.5$ sodium current were assessed using the whole-cell patch-clamp technique in transfected CHO cells. As described in Methods, bicistronic expression vectors encoding a reporter (GFP or DsRed) with or without β subunits were cotransfected with expression vector encoding $\text{Na}_v1.5$. Currents were compared in cells transfected with *SCN5A* plus WT, mutant, or both β subunits.

Figure 4A shows representative current traces in cells expressing $\text{Na}_v1.5$ alone and $\text{Na}_v1.5$ plus WT or mutant β1B (p.Trp179X β1B) or their combination; current densities at -30 mV are summarized in Figure 4B. Coexpression of $\text{Na}_v1.5$ with WT β1B significantly increased sodium current density over $\text{Na}_v1.5$ alone, by 69%, while currents recorded with p.Trp179X β1B coexpression were no different from $\text{Na}_v1.5$ alone. Similarly, while coexpression of WT subunit with $\text{Na}_v1.5$ shifted the voltage dependence of both activation and inactivation to more negative potentials compared with those with $\text{Na}_v1.5$ alone, no such shift was observed with the mutant (Figure 4C

and Table 1). This result indicates that while WT β1B modulates $\text{Na}_v1.5$ gating (in a fashion similar to WT β1; see below), the mutant exerts no such effect. Coexpression of WT or mutant β1B with $\text{Na}_v1.5$ did not alter recovery from inactivation (Figure 4D and Table 1).

To examine whether expression of the mutant influences the effect of WT β1B on $\text{Na}_v1.5$ current (e.g., to produce a dominant negative action), cells were transfected with $\text{Na}_v1.5$ and varying amounts of WT and p.Trp179X β1B. Figure 4B shows that the sodium current increase over $\text{Na}_v1.5$ alone recorded with transfection of 1 μg of both β1B subunit constructs was identical to the increase with that of 1 μg of WT β1B. In addition, the increase in sodium current recorded with transfection of 0.5 μg of both β1B subunit constructs was 51% of that with 1 μg of β1B alone. These data indicate that p.Trp179X β1B does not exert a dominant negative effect on WT β1B function and further support the finding that the mutant, unlike WT, does not affect sodium channel function.

Figure 5A shows representative current traces of $\text{Na}_v1.5$ and $\text{Na}_v1.5$ coexpressed with WT and/or mutant β1 (p.Glu87Gln β1); current densities are summarized in Figure 5B. Coexpression of $\text{Na}_v1.5$ with WT β1 significantly increased sodium current density at -30 mV, by 76%, while coexpression with mutant β1 (p.Glu87Gln β1) did not increase the sodium current. The increase in sodium current recorded with coexpression of $\text{Na}_v1.5$ and 1 μg of both WT and p.Glu87Gln β1 (+20%) was markedly smaller than the increase with coexpression of $\text{Na}_v1.5$ with 1 μg WT β1 alone (+76%), indicating that this mutant exerts a dominant negative effect on WT β1 function. Figure 5C shows that WT β1 produced negative shifts in the voltage dependence of $\text{Na}_v1.5$ activation and inactivation similar to those observed with WT β1B. p.Glu87Gln β1 shifted the voltage dependence of inactivation to negative potentials (similar to WT β1) but did not alter the voltage dependence of activation (Table 2). Coexpression of WT or mutant β1 with $\text{Na}_v1.5$ did not alter recovery from inactivation (Figure 5D and Table 2).

Since Glu87 is located in a region of the protein common to both β1 and β1B, we also studied the effects of p.Glu87Gln β1B on $\text{Na}_v1.5$ current properties (Supplemental Figure 1 and Supplemental Table 1; supplemental material available online with this article; doi:10.1172/JCI33891DS1). While WT β1B increased $\text{Na}_v1.5$ current by 69% (Figure 4), p.Glu87Gln β1B did not increase the sodium current compared with $\text{Na}_v1.5$ alone. Similarly, WT β1B produced a negative shift in voltage dependence of both activation and inactivation (Table 1), while p.Glu87Gln β1B shifted only the voltage dependence of inactivation compared with $\text{Na}_v1.5$ alone. As with the other β subunit

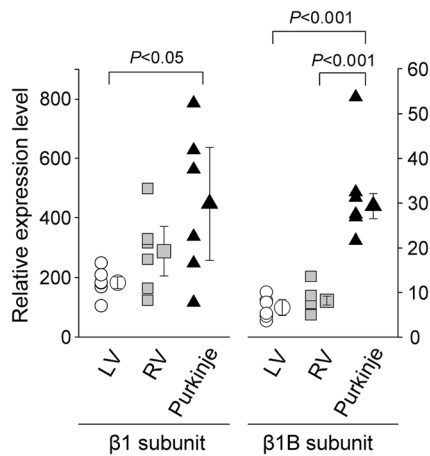


Figure 3

Expression profile of $\beta 1$ and $\beta 1B$ transcripts in nondiseased human ventricular tissue as determined by quantitative real-time PCR. Relative expression levels of the $\beta 1$ and $\beta 1B$ subunits are presented, normalized to those of *HPRT1* in LV (circles), RV (squares), and Purkinje fibers (triangles). Tissues for each group were collected from 6 human donors (nondiseased hearts, $n = 6$). Data points indicate the average of 2 measurements in each tissue sample. Larger symbols and error bars indicate median \pm median absolute deviation for all samples.

constructs studied, there was no change in recovery from inactivation. Thus, the effects of p.Glu87Gln were comparable in the $\beta 1$ and the $\beta 1B$ backbones.

Since Glu87 is located in a region of the protein common to both $\beta 1$ and $\beta 1B$, we also studied the effects of p.Glu87Gln $\beta 1B$ on $Na_V1.5$ current properties (Supplemental Figure 1 and Supplemental Table 1). While WT $\beta 1B$ increased $Na_V1.5$ current by 69% (Figure 4), p.Glu87Gln $\beta 1B$ did not increase the sodium current compared with $Na_V1.5$ alone. Similarly, WT $\beta 1B$ produced a negative shift in voltage dependence of both activation and inactivation (Table 1), while p.Glu87Gln $\beta 1B$ shifted only the voltage dependence of inactivation compared with $Na_V1.5$ alone. As with the other β subunit constructs studied, there was no change in recovery from inactivation. Thus, the effects of p.Glu87Gln were comparable in the $\beta 1$ and the $\beta 1B$ backbones.

activation (Table 1), while p.Glu87Gln $\beta 1B$ shifted only the voltage dependence of inactivation compared with $Na_V1.5$ alone. As with the other β subunit constructs studied, there was no change in recovery from inactivation. Thus, the effects of p.Glu87Gln were comparable in the $\beta 1$ and the $\beta 1B$ backbones.

Discussion

In this study, we provide what we believe to be the first report of mutations in *SCN1B* sequences encoding the $\beta 1$ and $\beta 1B$ transcript variants in patients with conduction disease and/or Brugada syndrome. Further, we provide new data indicating that $\beta 1$ and $\beta 1B$ transcripts in the heart vary by region; greater expression in Purkinje fibers is consistent with the conduction system phenotype we describe in mutation carrier patients. Finally, we demonstrate that the $\beta 1$ and $\beta 1B$ variants modulate function of the major cardiac sodium channel α subunit $Na_V1.5$ and that the identified *SCN1B* mutations blunt or inhibit this effect.

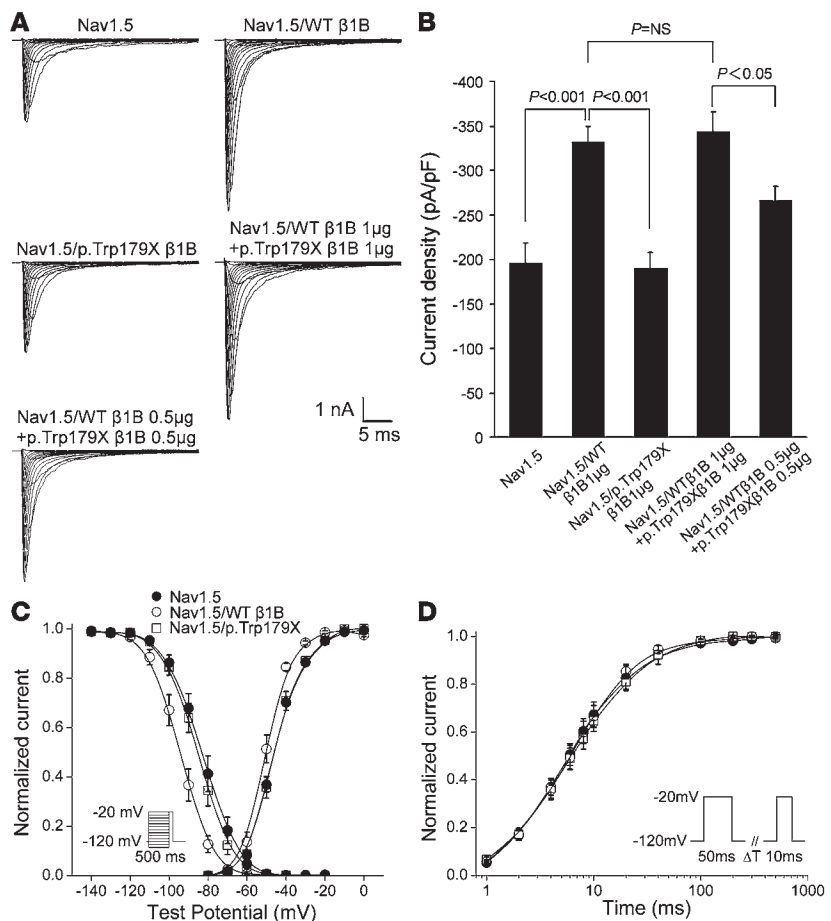


Figure 4

Electrophysiological characteristics of the p.Trp179X $\beta 1B$ mutant. (A) Representative traces of sodium current demonstrating an increase in sodium current with WT but not mutant subunit. (B) Sodium current density at -30 mV for $Na_V1.5$ alone ($n = 29$), $Na_V1.5$ coexpressed with WT $\beta 1B$ ($n = 28$), $Na_V1.5$ coexpressed with p.Trp179X $\beta 1B$ ($n = 18$), $Na_V1.5$ coexpressed with WT $\beta 1B$ plus p.Trp179X $\beta 1B$ ($1 \mu g$ for each; $n = 14$), and $Na_V1.5$ coexpressed with WT $\beta 1B$ plus p.Trp179X $\beta 1B$ ($0.5 \mu g$ for each; $n = 10$). (C) Voltage dependence of activation and inactivation. Filled circles, open circles, and squares indicate $Na_V1.5$ alone, $Na_V1.5$ coexpressed with WT $\beta 1B$, and $Na_V1.5$ coexpressed with p.Trp179X $\beta 1B$, respectively. The pulse protocol used to study the voltage dependence of inactivation is shown in the inset. (D) Recovery from inactivation. Biophysical properties are provided in Table 1.



Table 1

Biophysical parameters of WT and mutant $\beta 1B$

	Voltage dependence of activation			Voltage dependence of inactivation			Recovery from inactivation		
	$V_{1/2}$, mV	k , mV	n	$V_{1/2}$, mV	k , mV	n	τ_i , ms (amplitude, %) ^A	τ_s , ms (amplitude, %) ^A	n
Nav1.5	-46.2 ± 1.0	7.1 ± 0.4	29	-83.8 ± 1.8	7.6 ± 0.2	17	7.7 ± 1.1 (87.2 ± 1.1)	56.4 ± 9.8 (11.6 ± 1.0)	12
Nav1.5/WT $\beta 1B$	-50.6 ± 0.7 ^B	6.3 ± 0.3	28	-94.2 ± 1.3 ^A	7.6 ± 0.2	14	7.4 ± 1.0 (86.5 ± 1.2)	43.3 ± 8.6 (13.1 ± 1.1)	14
Nav1.5/p.Trp179X $\beta 1B$	-46.3 ± 1.3 ^C	6.5 ± 0.4	18	-85.2 ± 2.0 ^B	6.6 ± 0.3	15	8.2 ± 1.0 (91.8 ± 1.1)	58.0 ± 11.9 (7.8 ± 1.0)	12

Values are shown as mean ± SEM. ^AThe percentages refer to the properties of the overall time constants contributed by the 2 components τ_i and τ_s . ^B $P < 0.01$ versus Nav1.5 alone. ^C $P < 0.01$ versus Nav1.5/WT $\beta 1B$.

The 3 mutations were identified in 3 probands with conduction disease and/or Brugada syndrome as well as in other family members with or without these arrhythmia phenotypes. Formal linkage analysis was not possible because the families are too small and penetrance is incomplete. Thus, evidence in support of disease causality of these mutations (beyond their identification in subjects with clinical phenotypes) includes the findings that both $\beta 1$ and $\beta 1B$ transcripts are expressed in heart and that the mutant subunits (p.Glu87Gln $\beta 1$, p.Glu87Gln $\beta 1B$, and p.Trp179X $\beta 1B$) did not increase Nav1.5 currents in heterologous expression experiments, while WT $\beta 1$ and $\beta 1B$ did. Incomplete penetrance, a well-recognized feature of the monogenic arrhythmia syndromes (12, 23), was observed. For *SCN5A* mutations linked to Brugada syndrome, penetrance as low as 12.5% has been described (24). A role for sex, age, and genetic modifiers (e.g., common polymorphisms) is suspected (5, 25, 26), but the mechanisms for this common clinical finding remain poorly understood.

Two types of mutations were identified. The c.536G→A and c.537G→A mutations in exon 3A both result in a stop codon at

position 179, predicted to generate a $\beta 1B$ protein lacking the transmembrane and cytoplasmic domains and thus unable to integrate into the sarcolemma and to associate with Nav1.5. Thus, the a priori assumption is that a mutation such as this will cause disease by simple haploinsufficiency. The electrophysiologic data support this idea, since coexpression of p.Trp179X $\beta 1B$ failed to increase Nav1.5 current and did not modulate the effect of the WT $\beta 1B$ protein. Furthermore, the voltage dependencies of activation and inactivation of Nav1.5 coexpressed with p.Trp179X $\beta 1B$ were the same as those for Nav1.5 alone, in contrast to the shifts observed with WT $\beta 1B$. While *Scn1b*-knockout mice display clear ECG changes (27), studies with young (17- to 18-day-old) heterozygotes identified no difference from WT. Since age-related changes in conduction are a recognized feature of cardiac conduction disease and conduction delay is one of the proposed mechanisms of Brugada syndrome (2, 28), aging may be important for the β subunit-mediated phenotype.

On the other hand, the c.259G→C mutation leads to an amino acid substitution (p.Glu87Gln) within the extracellular domain of the

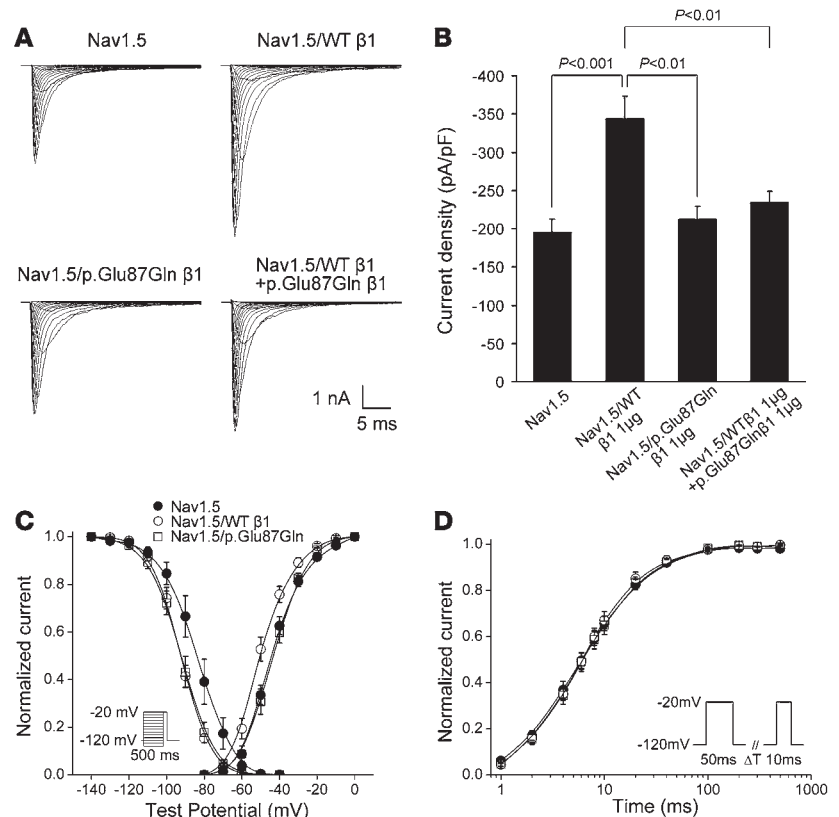


Figure 5 Electrophysiological characteristics of the p.Glu87Gln mutant. (A) Representative traces of sodium current. (B) Current density at -30 mV for Nav1.5 alone ($n = 13$), Nav1.5 coexpressed with WT $\beta 1$ ($n = 17$), Nav1.5 coexpressed with p.Glu87Gln $\beta 1$ ($n = 18$), and Nav1.5 coexpressed with WT $\beta 1$ plus p.Glu87Gln $\beta 1$ ($n = 15$). (C) Voltage dependence of activation and inactivation. Filled circles, open circles, and squares indicate Nav1.5 alone, Nav1.5 coexpressed with WT $\beta 1$, and Nav1.5 coexpressed with p.Glu87Gln $\beta 1$, respectively. (D) Recovery from inactivation. Biophysical properties are provided in Table 2.



Table 2
Biophysical parameters of WT and mutant $\beta 1$

	Voltage dependence of activation			Voltage dependence of inactivation			Recovery from inactivation		
	$V_{1/2}$, mV	k , mV	n	$V_{1/2}$, mV	k , mV	n	τ_i , ms (amplitude, %) ^A	τ_s , ms (amplitude, %) ^A	n
Nav1.5	-46.1 ± 1.7	7.8 ± 0.4	13	-85.1 ± 3.2	7.3 ± 0.5	12	8.2 ± 1.2 (88.2 ± 1.3)	52.4 ± 7.9 (11.0 ± 1.3)	9
Nav1.5/WT $\beta 1$	-50.6 ± 1.4^B	7.3 ± 0.4	17	-92.6 ± 1.4^A	6.4 ± 0.2	12	7.5 ± 1.1 (84.2 ± 1.3)	43.1 ± 4.6 (14.1 ± 1.3)	13
Nav1.5/p.Glu87Gln $\beta 1$	-44.9 ± 1.4^C	7.7 ± 0.4	18	-92.5 ± 1.7^A	6.8 ± 0.2	12	7.7 ± 1.1 (89.1 ± 1.1)	52.0 ± 9.5 (10.4 ± 1.1)	10

Values are shown as mean \pm SEM. ^AThe percentages refer to the properties of the overall time constants contributed by the 2 components τ_i and τ_s .

^B $P < 0.05$ versus Nav1.5 alone. ^C $P < 0.05$ versus Nav1.5 /WT $\beta 1$.

protein. The electrophysiological data demonstrate that the mutant subunit did modulate Nav1.5 gating (shift in the voltage dependence of inactivation, in either the $\beta 1$ or $\beta 1B$ background), supporting the idea that it associates with Nav1.5 at the cell surface. In addition, in contrast to the p.Trp179X $\beta 1B$, p.Glu87Gln did exert a dominant negative effect on the WT subunit. Thus, the 3 mutations lead to a decrease in Nav1.5 current through somewhat different mechanisms. This reduction of current is consistent with the conduction disease and Brugada syndrome phenotypes of the patients.

Normal impulse propagation in the atria, ventricles, and Purkinje network is critically dependent on normal sodium channel function. Dysfunction of the sodium channel leads to conduction delay, and loss-of-function mutations in *SCN5A* have been described in isolated conduction disease unassociated with structural heart disease (2, 3). Thus, our finding of *SCN1B* mutations associated with reduced sodium current in patients with conduction disease is consistent with previous studies of the mechanism of this disorder. The preferential expression of the $\beta 1$ and $\beta 1B$ transcripts in human Purkinje fibers further supports the prominent conduction delay seen as part of the clinical phenotypes.

Loss-of-function mutations in *SCN5A* were the first reported cause of the Brugada syndrome (4). These mutations reduce sodium current by reducing Nav1.5 cell surface expression and/or altering gating (4, 5, 29). A common view is that in epicardial cells, this reduction in sodium current produces marked action potential shortening, attributed to an “unopposed” early transient outward potassium current. By contrast, reduction of sodium current in endocardial cells is thought to produce only modest action potential shortening. The resultant increased heterogeneity of repolarization predisposes to rapid reentry, resulting in ventricular fibrillation (4, 30). A common feature in Brugada syndrome — consistent with reduced sodium current — is slowed conduction (28, 31). Indeed, an alternate proposed mechanism suggests that the characteristic right-precordial ST-segment elevation on the ECG and initiation of arrhythmias is attributable primarily to right-ventricular outflow tract conduction delay (28). The trend to higher expression levels of $\beta 1B$ in right ventricle may thus contribute to the Brugada syndrome phenotype.

This idea is further supported by functional studies in a single large kindred in which a *GPD1L* mutation was linked to Brugada syndrome: coexpression of mutant *GPD1L* with Nav1.5 was reported to decrease sodium current, consistent with the observation that loss-of-function mutations in *SCN5A* cause Brugada syndrome (12). In principle, reduction in L-type calcium current might also produce differential effects in epicardial and endocardial sites and thus cause Brugada syndrome; rare kindreds with this mechanism have now been described (14).

Conduction disease was observed in families 1 and 3, while in family 2, mutation carriers presented either solely with conduction disease or conduction disease in combination with ECGs typical of Brugada syndrome. This phenomenon of overlapping clinical phenotypes is common in individuals with *SCN5A* mutations leading to loss of sodium channel function (6, 7), and conversely, in vitro electrophysiologic analysis of *SCN5A* mutations linked to Brugada syndrome or isolated conduction disease consistently reveals loss of Nav1.5 channel function (2, 4). Indeed, a single mutation segregating in a given family can lead to conduction disease in some family members and Brugada syndrome in others (6, 7). What determines the ultimate phenotype — Brugada syndrome versus isolated conduction disease — is unknown. Sex, age, and genetic modifiers (e.g., common polymorphisms) have been proposed as modulators of the clinical phenotypes (5, 25, 26).

The reported effects of $\beta 1$ on Nav1.5 channels are controversial (32). Some groups have reported that $\beta 1$ increases Nav1.5 currents with or without affecting voltage dependence or channel kinetics, while others have reported no effect of $\beta 1$ on Nav1.5 current (20, 33–37). The $\beta 1B$ variant has to date only been studied in coexpression studies with the neuronal sodium channel Nav1.2 (encoded by *SCN2A*), where it was shown to increase sodium current and cause a small negative shift in voltage dependence of activation (19). In our experiments, WT $\beta 1$ and $\beta 1B$ had similar effects on Nav1.5 current: both increased sodium currents and led to hyperpolarizing (negative) shifts in voltage dependence of activation and inactivation.

Not only were the effects of the WT β subunits on Nav1.5 current similar, but the effects of the p.Glu87Gln mutation in the $\beta 1$ background (p.Glu87Gln $\beta 1$) were also similar to those in the $\beta 1B$ background (p.Glu87Gln $\beta 1B$). Although the $\beta 1$ and $\beta 1B$ variants share the same topology (an N-terminal extracellular immunoglobulin domain, a transmembrane domain, and a C-terminal cytoplasmic domain), their sequence identity is limited to the extracellular immunoglobulin domain; the C-terminal half of $\beta 1B$, residues 150–268, has only approximately 17% amino acid sequence identity with $\beta 1$ (19). Taken together, the data suggest that the molecular determinants of $\beta 1$ and $\beta 1B$ modulation of Nav1.5 cell-surface expression and gating likely reside in the extracellular immunoglobulin domain. This is in line with previous studies of skeletal muscle (Nav1.4 encoded by *SCN4A*) and neuronal (Nav1.2) sodium channel α subunits that have shown that deletion of the intracellular domain of the $\beta 1$ subunit has no effect on its modulation of α subunit function, whereas deletions within the extracellular domain block modulation (38–40). Alternatively, specific residues may not be as important as preservation of overall structural motifs, as suggested by the data of Zimmer



and Benndorf, who reported that the $\beta 1$ subunit modulates $\text{Nav}1.5$ via the membrane anchor plus additional intracellular or extracellular regions (41).

In addition to modulation of sodium channel α subunit expression and function, other roles have been suggested for β subunits: these include acting as adhesion molecules or as participants in signal transduction (16, 32). The different transmembrane and C-terminal domains of $\beta 1$ and $\beta 1B$ might therefore lead to participation in different signaling pathways. For instance, phosphorylation of the tyrosine at position 181 of the $\beta 1$ C terminus regulates its interaction with ankyrin-G (42), which is thought to be critical for ankyrin-G localization within cardiomyocytes (intercalated discs versus T tubules). $\beta 1B$ lacks this tyrosine in its C-terminal domain, so a role for $\beta 1B$ as a modulator of this function seems less likely.

Another mechanism regulating function of β subunits is the potential for cleavage by β -site amyloid precursor protein–cleaving enzyme (BACE1) and γ -secretase, resulting in the release of the N- and C-terminal fragments (43). The processed C-terminal fragment of $\beta 2$ and $\beta 4$ has been reported to be associated with cell adhesion, migration, and morphogenesis in neuronal cells as well as regulation of the expression level of the neuronal sodium channel $\text{Nav}1.1$ (44–46). Thus, p.Trp179X $\beta 1B$ may result in absence of functions depending on the generation of a β subunit C-terminal fragment by BACE1. However, a role for BACE1 cleavage has not been studied in either human $\beta 1$ subunit or cardiomyocytes, and the cleavage site located at the common juxtamembrane domain in $\beta 1$ and $\beta 1B$ is not conserved between human and mice (19, 43).

Mutations in *SCN1B* have been previously reported in generalized epilepsy with febrile seizures plus (47), and $\beta 1$ -null mice exhibit a severe seizure disorder and die at approximately 3 weeks of age (48). In addition, these mice exhibit bradycardia and prolonged rate-corrected QT intervals (27). These changes suggest that $\beta 1$ plays an important role in the murine heart, although it is possible that the changes are a consequence of the severe overall developmental phenotype in this model (48). To our knowledge, defects in cardiac function have not been investigated in *SCN1B* mutation carriers presenting with epilepsy (32, 49). Conversely, we have observed no neurological phenotype in our patients. Four *SCN1B* mutations have been linked to epilepsy to date (47, 49, 50), all of which localize to the extracellular immunoglobulin-like fold of the protein, as does the p.Glu87Gln mutation reported here. One additional possible link between the cardiac and neurological phenotypes associated with $\beta 1$ mutations is the syndrome of sudden unexpected death in epilepsy (SUDEP) (51), where a role for cardiac bradyarrhythmias has been proposed (52).

To date, *SCN5A* mutations are the most common cause identified in cases of Brugada syndrome, and *SCN5A* is the only identified causative gene in conduction disease (2, 11). However, *SCN5A* mutations are not identified in the majority of patients, and it has been reported that the frequency of mutations in other implicated genes (*CACNA1C*, *CACNB2b*, *GPD1L*) is also low in Brugada syndrome (12–14). In this study, *SCN1B* mutations were identified in less than 1% of probands with Brugada syndrome and less than 5% of probands with conduction disease and thus account for a small subset of these inherited arrhythmic syndromes.

A conventional heterologous mammalian expression system was used for functional assessment of the mutations. The environment in this approach is different from that in native cardiomyocytes, and other proteins known to associate with the sodium channel complex, such as other β subunits, are generally absent. Despite

these limitations, the in vitro characteristics of the mutations were concordant with the phenotype observed in the patients, which, in combination with the genetic data presented, supports the hypothesis of a causal relationship between the mutations and disease.

In summary, we have for the first time to our knowledge identified *SCN1B* mutations in families with conduction disease and Brugada syndrome. We have shown expression of the $\beta 1$ subunit transcript and the alternate $\beta 1B$ subunit transcript variant in human heart and demonstrated reduced $\text{Nav}1.5$ sodium current as a result of loss or altered β subunit modulation of $\text{Nav}1.5$ current. These findings implicate *SCN1B* as a disease gene for human arrhythmia susceptibility.

Methods

Study populations. The study populations consisted of: (a) unrelated Brugada syndrome probands identified and characterized at the Academic Medical Center, Amsterdam ($n = 38$), l'institut du thorax, Nantes, ($n = 216$), and the Niigata University Graduate School of Medical and Dental Sciences ($n = 28$); and (b) patients with cardiac conduction disease were identified and characterized at the Academic Medical Center ($n = 2$), l'institut du thorax ($n = 39$), and Ege University School of Medicine ($n = 3$). The study was performed according to a protocol approved by the Medical Ethical Committee, Academic Medical Center, Amsterdam; Comité de Protection des Personnes, Nantes; Ege University Research Ethics Committee; and Medical Research Ethics Committee, Niigata University Graduate School of Medical and Dental Sciences. Informed consent was obtained from all patients. Coding region and splice site mutations in *SCN5A* had been previously excluded in all probands by single-strand confirmation polymorphism analysis, denaturing HPLC sequencing, or direct sequencing using primers in flanking intronic sequences.

Mutation analysis. Probands with Brugada syndrome and cardiac conduction disease were screened for mutations in regions of the *SCN1B* gene encoding $\beta 1$ and $\beta 1B$, except for Japanese probands, who were screened only in the regions of *SCN1B* gene encoding $\beta 1B$. Screening for mutations was performed by PCR amplification of coding regions and flanking intronic sequences, followed by direct sequencing of amplicons on an ABI PRISM 3730 DNA Sequence Detection System (Applied Biosystems). Primer sequences are listed in Supplemental Table 2.

Control populations. We screened randomly selected and unrelated white Dutch individuals ($n = 176$); white individuals ($n = 702$) selected from the KORA S4 survey, which included population-based southern German individuals ($n = 4,261$) surveyed between 1999 and 2001 (53); unrelated white Turkish individuals ($n = 150$); and 4 different ethnic groups (white, African American, Hispanic, Asian; $n = 94$ for each group) from the Coriell Cell Repositories. The Coriell samples were resequenced as described above by the J. Craig Venter Institute through the NHLBI DNA Resequencing and Genotyping Program. The other control samples were genotyped at the identified mutation sites.

Subunit mRNA abundances in human cardiac tissue. Real-time RT-PCR was used to quantify subunit abundances. Assays were conducted in nondiseased human hearts obtained from the University of Szeged, Szeged, Hungary, that were technically unusable for transplantation based on logistic considerations (54). Before cardiac explantation, organ donor patients did not receive medication except dobutamine, furosemide, and plasma expanders. The investigations conformed to the principles outlined in the Helsinki Declaration of the World Medical Association. All experimental protocols were approved by the Ethical Review Board of the Medical Center of the University of Szeged (no. 51-57/1997 OEJ). The left ventricles from 6 donors and the right ventricles from 6 donors were dissected and stored in cardioplegic solution at 4°C for approximately 4–8 hours before being



frozen in liquid nitrogen. Purkinje fiber mRNA was extracted from false tendons dissected from the ventricles of 6 donors. Further information on the donors is presented in Supplemental Table 3.

Total RNA from each cardiac sample was isolated and DNase treated with the RNeasy Fibrous Tissue Mini Kit (QIAGEN) following the manufacturer's instructions. The quality of total RNA was assessed with PAGE (2100 Bioanalyzer; Agilent Technologies). Absence of genomic DNA contamination was verified by PCR. First-strand cDNA was synthesized from 2 μ g total RNA with High-Capacity cDNA Archive Kit (Applied Biosystems). Real-time PCR was performed on a TaqMan system with predesigned 6-carboxyfluorescein-labeled (FAM-labeled) fluorogenic TaqMan probe and primers for β 1, custom-designed TaqMan probe and primers for β 1B (located in the retained segment of intron 3), and 1 \times TaqMan Universal PCR Master Mix (Applied Biosystems). PCR efficiency of the β 1 and β 1B fluorescent probes was estimated at approximately 98%. After 2 minutes at 50°C and 10 minutes at 95°C, 40 cycles of amplification were performed with the ABI PRISM 7900HT Sequence Detection System (Applied Biosystems). Data were collected with instrument spectral compensation by Applied Biosystems SDS 2.1 software and analyzed with the Ct relative quantification method (55). Fluorescence signals were normalized to the housekeeping gene hypoxanthine phosphoribosyl transferase 1 (*HPRT1*). For each sample, β 1 and β 1B transcripts were quantified in duplicate. The values were averaged and then used for the $2^{-\Delta Ct} \times 100$ calculation, where $2^{-\Delta Ct}$ corresponds to expression relative to *HPRT*. Primer and probe sequences are listed in Supplemental Table 4.

Generation of expression vectors. Full-length human β 1 cDNA (GenBank accession number NM_001037) subcloned into a bicistronic vector also carrying the cDNA for enhanced eGFP (pEGFP-IRES; BD Biosciences – Clontech) was supplied by Alfred George Jr. (Vanderbilt University, Nashville, Tennessee, USA). Full-length human β 1B cDNA (GenBank accession number NM_199037) was cloned from human ventricular mRNA, supplied by Katherine Murray (Vanderbilt University). The β 1B cDNA was subcloned into a pEGFP-IRES vector (BD Biosciences – Clontech). Mutant constructs were prepared using the QuikChange II XL Site-Directed Mutagenesis Kit (Stratagene) according to the manufacturer's instructions. The inserts were subsequently sequenced to ensure that there was no other mutation besides the intended one.

Transient transfection in CHO cells. For functional analysis, cultured CHO cells were transiently transfected with the constructs described above using FuGENE 6 (Roche Applied Science). Constructs encoding β 1 or β 1B subunits (1 μ g, unless otherwise specified) were cotransfected with the pBK-CMV vector (1 μ g; Stratagene) encoding *SCN5A* (GenBank accession number NM_000335), supplied by Alfred George Jr. To study dominant negative effects, mutant β 1 or β 1B construct (0.5 μ g or 1 μ g) was cotransfected with the same amount of construct for WT β 1 or β 1B subunit that had been subcloned into a bicistronic vector also carrying cDNA for red fluorescent protein from *DiscoSoma* version T3 (pDsRed-IRES; supplied by Alfred George Jr.) along with *SCN5A* (1 μ g). When *SCN5A* was transfected without β subunits, the plasmid encoding the eGFP (pEGFP-IRES; BD Biosciences – Clontech) with no β subunit insert was cotransfected. Cells were grown for 48 hours after transfection before study.

Electrophysiology. Cells displaying green fluorescence were chosen for study; in experiments with transfection of both WT and mutant β subunits, cells displaying both green and red fluorescence were chosen. Sodium currents were measured at room temperature using the whole-cell configuration of the patch-clamp technique with an Axopatch 200B amplifier (Molecular Devices). The extracellular bath solution contained (in mmol/l): 145 NaCl, 4.0 KCl, 1.0 MgCl₂, 1.8 CaCl₂, 10 glucose, 10 HEPES, pH 7.4 (NaOH). Patch pipettes (~1.5 M Ω) contained (in mmol/l): 10 NaF, 110 CsF, 20 CsCl, 10 EGTA, and 10 HEPES, pH 7.4 (CsOH). Currents were filtered at 5 kHz and digitized at 50 kHz. Cell capacitance and series resistance were compensated for by at

least 80%. Voltage control, data acquisition, and analysis were accomplished using pCLAMP 9.2 and Clampfit 9.2 software (Molecular Devices).

Sodium current properties were determined by voltage clamp protocols as shown in the relevant figures. Cells were held at -120 mV, and currents were elicited with 50-ms depolarizing pulses from -80 to 60 mV in 10-mV increments. Voltage dependence of inactivation was studied using 500-ms prepulses from -120 to -20 mV in 10-mV increments, followed by a test pulse to -20 mV. The rate of recovery from inactivation was examined by 50-ms conditioning pulse to -20 mV from a holding potential of -120 mV, followed by a varying recovery duration and a 10-ms test pulse to -20 mV. All currents were normalized to cell capacitance. The voltage dependence of sodium current was determined by fitting a Boltzmann function ($y = [1 + \exp\{(V - V_{1/2}) / k\}]^{-1}$), yielding the voltage required to achieve half-maximal conductance or channel availability ($V_{1/2}$) and slope factor (k). The time constants of recovery from inactivation were determined using a double-exponential function ($y = A_f[1 - \exp(-t / \tau_f)] + A_s[1 - \exp(-t / \tau_s)]$), where τ_f and τ_s are the time constants of fast and slow components, and A_f and A_s are the fractions of the fast and slow components.

Statistics. Electrophysiological data are expressed as mean \pm SEM. Gene expression data are expressed as median \pm median absolute deviation. All statistical analyses were conducted with SPSS version 12.0. To test for significant differences among groups, an unpaired 2-tailed *t* test or ANOVA was used. The level of statistical significance was $P < 0.05$.

Acknowledgments

We thank Leander Beekman, Peter van Tintelen, Arie O. Verkerk, Carol Ann Remme, Alfred George Jr., Katherine Murray, Sabina Kupersmidt, Kai Liu, Sameer Chopra, Nathalie Gaborit, Satoru Komura, Mahmut Akyol, and Moritz Sinner for their contributions to performing and/or analyzing this work and for helpful discussions. This work was supported by grants from the NIH (HL46681 and HL65962 to D.M. Roden), a Fondation Leducq Trans-Atlantic Network of Excellence grant (05 CVD 01, Preventing Sudden Death, to D. Escande, J.-J. Schott, A.M. Wilde, S. Käb, and D.M. Roden), Netherlands Heart Foundation grant 2003T302 (to A.A.M. Wilde), the Interuniversity Cardiology Institute of The Netherlands (project 27, to A.A.M. Wilde), Agence Nationale de la Recherche grant 05-MRAR-028 (to J.-J. Schott), Agence Nationale de la Recherche grants 05-MRAR-028 and 06-MRAR-022 (to J.-J. Schott), German Federal Ministry of Education and Research (BMBF) grants 01GI0204, 01GS0499, 01GI0204, and 01GR0103 (to S. Käb, A. Pfeufer, and H.-E. Wichmann), and a Sumitomo Life Social Foundation grant (to H. Watanabe). The KORA platform is funded by the BMBF and by the State of Bavaria. Resequencing of Coriell samples was performed by the J. Craig Venter Institute through the NHLBI Resequencing and Genotyping Program. We also thank Andras Varro (University of Szeged) for providing the human tissues. C.R. Bezzina is an Established Investigator of The Netherlands Heart Foundation (grant 2005/T024).

Received for publication September 11, 2007, and accepted in revised form March 19, 2008.

Address correspondence to: Connie R. Bezzina, Heart Failure Research Center, Department of Experimental Cardiology, L2-108-1, Meibergdreef 15, 1105 AZ Amsterdam, The Netherlands. Phone: 31-20-5665403; Fax: 31-20-6976177; E-mail: C.R.Bezzina@amc.uva.nl.

Hiroshi Watanabe, Tamara T. Koopmann, and Solena Le Scouarnec contributed equally to this work.



1. Wang, Q., et al. 1995. SCN5A mutations associated with an inherited cardiac arrhythmia, long QT syndrome. *Cell*. **80**:805–811.
2. Schott, J.J., et al. 1999. Cardiac conduction defects associate with mutations in SCN5A. *Nat. Genet.* **23**:20–21.
3. Tan, H.L., et al. 2001. A sodium-channel mutation causes isolated cardiac conduction disease. *Nature*. **409**:1043–1047.
4. Chen, Q., et al. 1998. Genetic basis and molecular mechanism for idiopathic ventricular fibrillation. *Nature*. **392**:293–296.
5. Tan, H.L., Bezzina, C.R., Smits, J.P., Verkerk, A.O., and Wilde, A.A. 2003. Genetic control of sodium channel function. *Cardiovasc. Res.* **57**:961–973.
6. Bezzina, C., et al. 1999. A single Na⁺ channel mutation causing both long-QT and Brugada syndromes. *Circ. Res.* **85**:1206–1213.
7. Kyndt, F., et al. 2001. Novel SCN5A mutation leading either to isolated cardiac conduction defect or Brugada syndrome in a large French family. *Circulation*. **104**:3081–3086.
8. Grant, A.O., et al. 2002. Long QT syndrome, Brugada syndrome, and conduction system disease are linked to a single sodium channel mutation. *J. Clin. Invest.* **110**:1201–1209.
9. Valdivia, C.R., et al. 2002. A novel SCN5A arrhythmia mutation, M1766L, with expression defect rescued by mexiletine. *Cardiovasc. Res.* **55**:279–289.
10. Remme, C.A., et al. 2006. Overlap syndrome of cardiac sodium channel disease in mice carrying the equivalent mutation of human SCN5A-1795insD. *Circulation*. **114**:2584–2594.
11. Shimizu, W., Aiba, T., and Kamakura, S. 2005. Mechanisms of disease: current understanding and future challenges in Brugada syndrome. *Nat. Clin. Pract. Cardiovasc. Med.* **2**:408–414.
12. London, B., et al. 2007. Mutation in glycerol-3-phosphate dehydrogenase 1 like gene (GPD1-L) decreases cardiac Na⁺ current and causes inherited arrhythmias. *Circulation*. **116**:2260–2268.
13. Koopmann, T.T., et al. 2007. Exclusion of multiple candidate genes and large genomic rearrangements in SCN5A in a Dutch Brugada syndrome cohort. *Heart Rhythm*. **4**:752–755.
14. Antzelevitch, C., et al. 2007. Loss-of-function mutations in the cardiac calcium channel underlie a new clinical entity characterized by ST-segment elevation, short QT intervals, and sudden cardiac death. *Circulation*. **15**:442–449.
15. Moric, E., et al. 2003. The implications of genetic mutations in the sodium channel gene (SCN5A). *Europace*. **5**:325–334.
16. Isom, L.L. 2001. Sodium channel beta subunits: anything but auxiliary. *Neuroscientist*. **7**:42–54.
17. Abriel, H., and Kass, R.S. 2005. Regulation of the voltage-gated cardiac sodium channel Nav1.5 by interacting proteins. *Trends Cardiovasc. Med.* **15**:35–40.
18. Kazen-Gillespie, K.A., et al. 2000. Cloning, localization, and functional expression of sodium channel beta1A subunits. *J. Biol. Chem.* **275**:1079–1088.
19. Qin, N., et al. 2003. Molecular cloning and functional expression of the human sodium channel beta1B subunit, a novel splicing variant of the beta1 subunit. *Eur. J. Biochem.* **270**:4762–4770.
20. Nuss, H.B., et al. 1995. Functional association of the beta 1 subunit with human cardiac (hH1) and rat skeletal muscle (mu 1) sodium channel alpha subunits expressed in *Xenopus* oocytes. *J. Gen. Physiol.* **106**:1171–1191.
21. Wilde, A.A., et al. 2002. Proposed diagnostic criteria for the Brugada syndrome: consensus report. *Circulation*. **106**:2514–2519.
22. Dickinson, D.F. 2005. The normal ECG in childhood and adolescence. *Heart*. **91**:1626–1630.
23. Priori, S.G., Napolitano, C., and Schwartz, P.J. 1999. Low penetrance in the long-QT syndrome: clinical impact. *Circulation*. **99**:529–533.
24. Priori, S.G., et al. 2000. Clinical and genetic heterogeneity of right bundle branch block and ST-segment elevation syndrome: a prospective evaluation of 52 families. *Circulation*. **102**:2509–2515.
25. Viswanathan, P.C., Benson, D.W., and Balsler, J.R. 2003. A common SCN5A polymorphism modulates the biophysical effects of an SCN5A mutation. *J. Clin. Invest.* **111**:341–346.
26. Bezzina, C.R., et al. 2006. Common sodium channel promoter haplotype in Asian subjects underlies variability in cardiac conduction. *Circulation*. **113**:338–344.
27. Lopez-Santiago, L.F., et al. 2007. Sodium channel *Scn1b* null mice exhibit prolonged QT and RR intervals. *J. Mol. Cell. Cardiol.* **43**:636–647.
28. Meregalli, P.G., Wilde, A.A., and Tan, H.L. 2005. Pathophysiological mechanisms of Brugada syndrome: depolarization disorder, repolarization disorder, or more? *Cardiovasc. Res.* **67**:367–378.
29. Baroudi, G., et al. 2001. Novel mechanism for Brugada syndrome: defective surface localization of an SCN5A mutant (R1432G). *Circ. Res.* **88**:e78–e83.
30. Yan, G.X., and Antzelevitch, C. 1999. Cellular basis for the Brugada syndrome and other mechanisms of arrhythmogenesis associated with ST-segment elevation. *Circulation*. **100**:1660–1666.
31. Antzelevitch, C., et al. 2005. Brugada syndrome: report of the second consensus conference: endorsed by the Heart Rhythm Society and the European Heart Rhythm Association. *Circulation*. **111**:659–670.
32. Meadows, L.S., and Isom, L.L. 2005. Sodium channels as macromolecular complexes: implications for inherited arrhythmia syndromes. *Cardiovasc. Res.* **67**:448–458.
33. Qu, Y., et al. 1995. Modulation of cardiac Na⁺ channel expression in *Xenopus* oocytes by beta 1 subunits. *J. Biol. Chem.* **270**:25696–25701.
34. Ko, S.H., Lenkowski, P.W., Lee, H.C., Mounsey, J.P., and Patel, M.K. 2005. Modulation of Na(v)1.5 by beta1- and beta3-subunit co-expression in mammalian cells. *Pflugers Arch.* **449**:403–412.
35. Johnson, D., Montpetit, M.L., Stocker, P.J., and Bennett, E.S. 2004. The sialic acid component of the beta1 subunit modulates voltage-gated sodium channel function. *J. Biol. Chem.* **279**:44303–44310.
36. Fahmi, A.I., et al. 2001. The sodium channel beta-subunit SCN3b modulates the kinetics of SCN5a and is expressed heterogeneously in sheep heart. *J. Physiol.* **537**:693–700.
37. Makita, N., Bennett, P.B., Jr., and George, A.L., Jr. 1994. Voltage-gated Na⁺ channel beta 1 subunit mRNA expressed in adult human skeletal muscle, heart, and brain is encoded by a single gene. *J. Biol. Chem.* **269**:7571–7578.
38. Chen, C., and Cannon, S.C. 1995. Modulation of Na⁺ channel inactivation by the beta 1 subunit: a deletion analysis. *Pflugers Arch.* **431**:186–195.
39. McCormick, K.A., et al. 1998. Molecular determinants of Na⁺ channel function in the extracellular domain of the beta1 subunit. *J. Biol. Chem.* **273**:3954–3962.
40. McCormick, K.A., Srinivasan, J., White, K., Scheuer, T., and Catterall, W.A. 1999. The extracellular domain of the beta1 subunit is both necessary and sufficient for beta1-like modulation of sodium channel gating. *J. Biol. Chem.* **274**:32638–32646.
41. Zimmer, T., and Benndorf, K. 2002. The human heart and rat brain IIA Na⁺ channels interact with different molecular regions of the beta1 subunit. *J. Gen. Physiol.* **120**:887–895.
42. Malhotra, J.D., Thyagarajan, V., Chen, C., and Isom, L.L. 2004. Tyrosine-phosphorylated and nonphosphorylated sodium channel beta1 subunits are differentially localized in cardiac myocytes. *J. Biol. Chem.* **279**:40748–40754.
43. Wong, H.K., et al. 2005. beta Subunits of voltage-gated sodium channels are novel substrates of beta-site amyloid precursor protein-cleaving enzyme (BACE1) and gamma-secretase. *J. Biol. Chem.* **280**:23009–23017.
44. Kim, D.Y., Ingano, L.A., Carey, B.W., Pettinelli, W.H., and Kovacs, D.M. 2005. Presenilin/gamma-secretase-mediated cleavage of the voltage-gated sodium channel beta2-subunit regulates cell adhesion and migration. *J. Biol. Chem.* **280**:23251–23261.
45. Kim, D.Y., et al. 2007. BACE1 regulates voltage-gated sodium channels and neuronal activity. *Nat. Cell Biol.* **9**:755–764.
46. Miyazaki, H., et al. 2007. BACE1 modulates filopodia-like protrusions induced by sodium channel beta4 subunit. *Biochem. Biophys. Res. Commun.* **361**:43–48.
47. Wallace, R.H., et al. 1998. Febrile seizures and generalized epilepsy associated with a mutation in the Na⁺-channel beta1 subunit gene SCN1B. *Nat. Genet.* **19**:366–370.
48. Chen, C., et al. 2004. Mice lacking sodium channel beta1 subunits display defects in neuronal excitability, sodium channel expression, and nodal architecture. *J. Neurosci.* **24**:4030–4042.
49. Scheffer, I.E., et al. 2007. Temporal lobe epilepsy and GEFS+ phenotypes associated with SCN1B mutations. *Brain*. **130**:100–109.
50. Audenaert, D., et al. 2003. A deletion in SCN1B is associated with febrile seizures and early-onset absence epilepsy. *Neurology*. **61**:854–856.
51. Nashef, L., Hindocha, N., and Makoff, A. 2007. Risk factors in sudden death in epilepsy (SUDEP): the quest for mechanisms. *Epilepsia*. **48**:859–871.
52. Rugg-Gunn, F.J., Simister, R.J., Squirrell, M., Holdright, D.R., and Duncan, J.S. 2004. Cardiac arrhythmias in focal epilepsy: a prospective long-term study. *Lancet*. **364**:2212–2219.
53. Wichmann, H.E., Gieger, C., and Illig, T. 2005. KORA-gen — resource for population genetics, controls and a broad spectrum of disease phenotypes. *Gesundheitswesen*. **67**(Suppl. 1):S26–S30.
54. Gaborit, N., Le Bouter, S., Szuts, V., Varro, A., Escande, D., Nattel, S., and Demolombe, S. 2007. Regional and tissue specific transcript signatures of ion channel genes in the non-diseased human heart. *J. Physiol.* **582**:675–693.
55. Livak, K.J., and Schmittgen, T.D. 2001. Analysis of relative gene expression data using real-time quantitative PCR and the 2(-Delta Delta C(T)) Method. *Methods*. **25**:402–408.